



RESEARCH ARTICLE

Trace elements as potential modulators of puberty-induced amelioration of oxidative stress and inflammation in childhood obesity

Álvaro González-Domínguez¹ | Jesús Domínguez-Riscart^{1,2} |
 María Millán-Martínez^{3,4} | Rosa María Mateos-Bernal^{1,5}  |
 Alfonso María Lechuga-Sancho^{1,2,6} | Raúl González-Domínguez¹ 

¹Instituto de Investigación e Innovación Biomédica de Cádiz (INiBICA), Hospital Universitario Puerta del Mar, Universidad de Cádiz, Cádiz, Spain

²Unidad de Endocrinología Pediátrica y Diabetes, Servicio de Pediatría, Hospital Universitario Puerta del Mar, Cádiz, Spain

³Associate Unit CSIC-University of Huelva "Atmospheric Pollution", Center for Research in Sustainable Chemistry – CIQSO, University of Huelva, Huelva, Spain

⁴Department of Chemistry, Faculty of Experimental Sciences, University of Huelva, Huelva, Spain

⁵Área de Bioquímica y Biología Molecular, Departamento de Biomedicina, Biotecnología y Salud Pública, Universidad de Cádiz, Cádiz, Spain

⁶Departamento Materno Infantil y Radiología, Facultad de Medicina, Universidad de Cádiz, Cádiz, Spain

Correspondence

Raúl González-Domínguez, Instituto de Investigación e Innovación Biomédica de Cádiz (INiBICA), Hospital Universitario Puerta del Mar, Universidad de Cádiz, 11009 Cádiz, Spain.
 Email: raul.gonzalez@inibica.es

Abstract

Although puberty is known to influence obesity progression, the molecular mechanisms underlying the role of sexual maturation in obesity-related complications remains largely unexplored. Here, we delve into the impact of puberty on the most relevant pathogenic hallmarks of obesity, namely oxidative stress and inflammation, and their association with trace element blood status. To this end, we studied a well-characterized observational cohort comprising prepubertal ($N = 46$) and pubertal ($N = 48$) children with obesity. From all participants, plasma and erythrocyte samples were collected and subjected to metallomics analysis and determination of classical biomarkers of oxidative stress and inflammation. Besides the expected raise of sexual hormones, pubertal children displayed better inflammatory and oxidative control, as reflected by lower levels of C-reactive protein and oxidative damage markers, as well as improved antioxidant defense. This was in turn accompanied by a healthier multielemental profile, with increased levels of essential elements involved in the antioxidant system and metabolic control (metalloproteins containing zinc, molybdenum, selenium, and manganese) and decreased content of potentially deleterious species (total copper, labile free iron). Therefore, our findings suggest that children with obesity have an exacerbated inflammatory and oxidative damage at early ages, which could be ameliorated during pubertal development by the action of trace element-mediated buffering mechanisms.

Abbreviations: 6PGDH, 6-phosphogluconate dehydrogenase; AUCg, area under the curve for glucose; AUCi, area under the curve for insulin; BMI, body mass index; CRP, C-reactive protein; E2, 17 β -estradiol; FSH, follicle-stimulating hormone; G6PDH, glucose-6-phosphate dehydrogenase; HMM, high molecular mass; HOMA-IR, homeostasis model assessment of insulin resistance; IGF-1, insulin-like growth factor; IR, insulin resistance; LH, luteinizing hormone; LMM, low molecular mass; OGTT, oral glucose tolerance test; T, testosterone; TBARS, thiobarbituric acid reactive substances; TIBC, total iron binding capacity.

This is an open access article under the terms of the [Creative Commons Attribution-NonCommercial-NoDerivs](https://creativecommons.org/licenses/by-nc-nd/4.0/) License, which permits use and distribution in any medium, provided the original work is properly cited, the use is non-commercial and no modifications or adaptations are made.

© 2023 The Authors. *BioFactors* published by Wiley Periodicals LLC on behalf of International Union of Biochemistry and Molecular Biology.

Funding information

INiBICA, Grant/Award Number: LII19/16IN-CO24; Instituto de Salud Carlos III, Grant/Award Numbers: CP21/00120, PI18/01316, PI22/01899

KEYWORDS

childhood obesity, inflammation, oxidative stress, puberty, trace elements

1 | INTRODUCTION

Childhood overweight and obesity have reached pandemic levels, with a prevalence that nowadays accounts for approximately 40 million children under the age of 5 years and more than 330 million children and adolescents aged from 5 to 19 years.¹ Not only its high prevalence, but also the concomitance of other adverse health consequences, make obesity at pediatric age a major public health issue. In this respect, oxidative stress and chronic low-grade inflammation have been proposed as pivotal molecular drivers of many of these obesity-related disorders.² Thus, it has been described that children with obesity exhibit a marked pro-inflammatory status (i.e., raised production of cytokines, abnormal white blood cell counts)³ and altered redox metabolism, this latter characterized by increased levels of lipid and protein oxidation markers as well as by impaired antioxidant defense.^{4,5} Moreover, obesity is also known to alter puberty progression, and puberty to influence obesity-related complications. Indeed, sexual hormones are important regulators of adipose tissue differentiation and distribution.⁶ Furthermore, pubertal children are prone to develop physiological insulin resistance (IR) compared to their prepubertal counterparts, being growth hormone and insulin-like growth factor (IGF-1) the primary mediators of this condition.⁷ On the other hand, it has been reported that sexual hormones, and especially estrogens, are involved in the modulation of oxidative stress^{8,9} and inflammation.¹⁰ Altogether, it seems clear that hormonal changes during puberty are crucial players in the progression of childhood obesity and related pathogenic events.

In this venue, trace elements are considered pivotal components of redox metabolism, the immune system, and hormone function.^{11–13} A few authors have previously investigated the association between childhood obesity, metabolic risk factors, and circulating metal concentrations,^{14–18} but the impact of puberty on these perturbations remains unexplored. In this work, we studied the influence of hormonal changes during puberty in modulating the oxidative and inflammatory milieu in childhood obesity, with a particular focus on metal metabolism regulation. To this end, we analyzed the multielemental profile, as well as classical biomarkers of oxidative stress and inflammation, in plasma and erythrocyte samples from an observational cohort comprising prepubertal and pubertal children with obesity. A high-throughput metallomics method was applied to determine, in a simple and fast manner, the total content of various trace elements and heavy metals, as well as their distribution

within high molecular mass (HMM, i.e., metalloproteins) and low molecular mass (LMM, i.e., free labile species) fractions. This methodology represents an excellent alternative to conventional chromatographic and electrophoretic approaches for metal speciation, which are more tedious, time-consuming, and prone to species interconversion during the separation process.

2 | EXPERIMENTAL PROCEDURES

2.1 | Study population and sample collection

Children and adolescents with obesity of both sexes, aged between 6 and 16 years, were recruited at “Hospital Universitario Puerta del Mar” (Cádiz, Spain). Obesity was diagnosed when presenting a body mass index (BMI) over two standard deviations (SDs) above the mean of the reference population, adjusted for sex and age.¹⁹ The Tanner scale was employed to stratify subjects in the prepubertal (Tanner = 1, $N = 46$) and pubertal (Tanner ≥ 2 , $N = 48$) groups. Children with other known chronic systemic diseases or suffering of acute infectious processes were not eligible for the study. The participants were subjected to an oral glucose tolerance test (OGTT), in the morning and after overnight fasting, with the aim to assess their carbohydrate metabolism. At baseline and along the OGTT curve (i.e., 30, 60, 90, and 120 min), venous blood samples were extracted using BD Vacutainer tubes and Advance vacuum system. Then, tubes were centrifuged for 10 min at 1500g and 4°C to obtain the plasma, and the resulting pellets were washed three times with cold saline solution (9 g/L NaCl, 4°C) to obtain the erythrocyte fraction (1500g, 4°C, 5 min). All the samples were aliquoted and stored at -80°C until analysis. The study was performed in accordance with the principles contained in the Declaration of Helsinki. The Ethical Committee of “Hospital Universitario Puerta del Mar” (Cádiz, Spain) approved the study protocol (Ref. PI22/01899), and all participants and/or legal guardians provided written informed consent.

2.2 | Anthropometric and biochemical variables

Anthropometric variables, including height, weight, and BMI were evaluated by pediatric endocrinologists. An

Alinity automatic analyzer (Abbot, Spain) was employed to determine blood levels of glucose and insulin along the OGTT experiment, as well as fasting levels of lipids (i.e., total cholesterol, high-density lipoprotein cholesterol, low-density lipoprotein cholesterol, triglycerides), hormones (i.e., growth hormone; insulin-like growth factor, IGF-1; luteinizing hormone, LH; follicle-stimulating hormone, FSH; 17 β -estradiol, E2; testosterone, T), iron metabolism-related variables (i.e., ferritin; transferrin; transferrin saturation; total iron binding capacity, TIBC; haptoglobin), and C-reactive protein (CRP). The homeostasis model assessment of insulin resistance (HOMA-IR) and the areas under the curve for glucose (AUCg) and insulin (AUCi) were calculated by applying the following formulas (1)–(3):

$$\text{HOMA-IR} = \frac{\text{Glucose 0} \times \text{Insulin 0} \times 0.055}{22.5} \quad (1)$$

$$\text{AUCg} = 0.25 \times \text{Glucose 0} + 0.5 \times \text{Glucose 30} + 0.75 \times \text{Glucose 60} + 0.5 \times \text{Glucose 120} \quad (2)$$

$$\text{AUCi} = 0.25 \times \text{Insulin 0} + 0.5 \times \text{Insulin 30} + 0.75 \times \text{Insulin 60} + 0.5 \times \text{Insulin 120} \quad (3)$$

2.3 | Determination of oxidative stress markers

Erythrocyte samples were subjected to spectrophotometric determinations for evaluating various oxidative stress markers, namely total antioxidant capacity, lipid peroxidation products, protein carbonyl groups, catalase activity, glutathione reductase activity, glucose-6-phosphate dehydrogenase (G6PDH) activity, and 6-phosphogluconate dehydrogenase (6PGDH) activity. To this end, the samples were analyzed in triplicate.

2.3.1 | Total antioxidant capacity

The total antioxidant capacity was evaluated using the method proposed by Erel based on the competition between o-dianisidine and the antioxidant species present in the sample for hydroxyl radicals.²⁰ To this end, 5 μ L of erythrocytes were mixed with 200 μ L of a buffer (75 mM Clark and Lubs buffer at pH 1.8) containing 10 mM o-dianisidine. After measuring the baseline absorbance at 444 nm, the reaction was triggered by adding 10 μ L of 75 mM H₂O₂ and incubating for 3 min. The difference between baseline and post-incubation absorbances is representative of the amount of antioxidant agents in the

sample. Results were expressed as μ mol of Trolox equivalents per mg of protein.

2.3.2 | Lipid peroxidation products

The formation of thiobarbituric acid reactive substances (TBARS) was measured according to the method described by Buege et al.²¹ Briefly, 100 μ L of diluted erythrocyte samples (1:1 v/v in water) were mixed with 400 μ L of the reaction solution, composed of 2.5 N HCl, 0.375% thiobarbituric acid (w/v), 15% trichloroacetic acid (w/v), and 0.01% butylated hydroxytoluene (w/v). Then, the mixture was heated at 100°C for 15 min and centrifuged at 900g for 5 min. The TBARS standard curve was prepared in the same way but without heating and centrifuging. Finally, 200 μ L of each sample were added to a 96-well microplate and the absorbance was recorded at 535 nm. Results were expressed as nmol of TBARS per mg of protein.

2.3.3 | Protein carbonyl groups

Carbonyl groups were determined following the method described by Levine et al.²² To this end, 100 μ L of erythrocytes were incubated with 400 μ L of 10 mM 2,4-dinitrophenylhydrazine (DNPH) dissolved in 2.5 N HCl for an hour in darkness. Then, proteins were purified by incubating with 500 μ L of 20% trichloroacetic acid for 5 min and further centrifugation for 10 min at 2000g and 4°C. The pellet was washed three times with 500 μ L of ethanol: ethyl acetate (1:1 v/v) and subsequently incubated with 250 μ L of 6 M guanidine hydrochloride (prepared in 20 mM KH₂PO₄, pH 2.3) during 15 min at 37°C for resuspension. Finally, the absorbance was registered at 370 nm in DNPH treated samples and at 280 nm in blanks. To estimate the protein content of the samples, a bovine serum albumin standard curve, prepared in 6 M HCl-guanidine, was used. Results were expressed as nmol of carbonyl groups per mg of protein.

2.3.4 | Catalase activity

As described by Aebi et al., catalase activity was measured by monitoring the decomposition rate of artificially added H₂O₂.²³ This method relies on the assumption that, at cytosolic level, exogenously added H₂O₂ is predominantly neutralized by catalase, whereas other peroxidases (e.g., glutathione peroxidase and peroxiredoxin 2) primarily operate in the erythrocyte membrane.²⁴ For

this purpose, 2 μL of diluted erythrocytes (1:100 v/v in water) were added to 200 μL of a 50 mM phosphate buffer (pH 7) containing 9.96 mM H_2O_2 . Then, the absorbance was measured at 240 nm during 2 min with readings every 10 s. For further calculations, the molar extinction coefficient for H_2O_2 was assumed to be $39.58 \text{ M}^{-1} \text{ cm}^{-1}$. The enzymatic activity was expressed as $\text{nmol H}_2\text{O}_2 \text{ min}^{-1}$ per mg of protein.

2.3.5 | Glutathione reductase activity

Glutathione reductase activity was determined following the NADPH oxidation rate.⁴ Briefly, 5 μL of erythrocyte samples were mixed with 150 μL of 0.1 M HEPES-NaOH buffer (pH 7.8, with 1 mM EDTA and 3 mM MgCl_2) containing 0.5 mM oxidized glutathione. Blanks were prepared in the same way but without adding glutathione. Then, 5 μL of 0.2 mM NADPH was added to start the reaction and the absorbance was measured at 340 nm for 2 min with readings every 10 s. For further calculations, the molar extinction coefficient for NADPH was assumed to be $6.22 \text{ mM}^{-1} \text{ cm}^{-1}$. The enzymatic activity was expressed as $\text{nmol NADP min}^{-1}$ per mg of protein.

2.3.6 | Dehydrogenase activities

The enzymatic activities of G6PDH and 6PGDH were estimated spectrophotometrically by quantifying the rate of NADP^+ reduction, as previously described.⁴ To this end, 5 μL of erythrocytes were added to 150 μL of a buffer containing 50 mM HEPES pH 7.6, 2 mM MgCl_2 , and 0.8 mM NADP^+ . Then, 20 μL of the substrates (glucose-6-phosphate and 6-phosphogluconate) were added to a final concentration of 5 mM to start the reaction. Finally, the absorbance was measured at 340 nm for 3 min with readings every 20 s. For further calculations, the molar extinction coefficient for NADP^+ was assumed to be $6.22 \text{ mM}^{-1} \text{ cm}^{-1}$. The enzymatic activity was expressed as $\text{nmol NADP min}^{-1}$ per mg of protein.

2.4 | Multielemental analysis of plasma and erythrocyte samples

Total metal contents were determined by simple dilution of plasma (150 μL) and erythrocyte (50 μL) samples to a final volume of 3 mL using an alkaline solution containing 2% 1-butanol (w/v), 0.05% EDTA (w/v), 0.05% Triton X-100 (w/v), 1% NH_4OH (w/v), and 1 $\mu\text{g/L}$ rhodium (internal standard). Furthermore, a second aliquot was employed to size-fractionate HMM and LMM metal

species following the method optimized by González-Domínguez et al.²⁵ To this end, 300 μL of cold acetone was added dropwise to 150/50 μL of plasma/erythrocytes, and the samples were then vortexed for 10 min at 4°C . After centrifuging at 10,000g for 10 min at 4°C , the supernatants were transferred to new tubes and taken to dryness using a SpeedVac system. Finally, dried supernatants (i.e., LMM fraction) and protein pellets (i.e., HMM fraction) were reconstituted in 3 mL of the above-described alkaline solution. Then, multielemental analyses were carried out in an Agilent 7900 inductively coupled plasma mass spectrometer (ICP-MS), equipped with nickel sampling and skimmer cones and with collision/reaction cell system (Agilent Technologies, Tokyo, Japan), using the operating conditions described elsewhere.²⁵ The isotopes monitored were ^{52}Cr , ^{53}Cr , ^{55}Mn , ^{56}Fe , ^{57}Fe , ^{59}Co , ^{63}Cu , ^{66}Zn , ^{77}Se , ^{78}Se , ^{82}Se , ^{95}Mo , ^{98}Mo , ^{103}Rh , ^{111}Cd , and ^{208}Pb . Multielemental calibration curves were prepared in alkaline solution within the concentration range 0.5–2500 $\mu\text{g/L}$, containing 1 $\mu\text{g/L}$ rhodium as the internal standard.

The method accuracy was validated by analyzing quality control (QC) samples, which were prepared by mixing equal aliquots of all the study samples and were subsequently spiked with all the metals under investigation at three concentration levels (0.5, 10, and 50 $\mu\text{g/L}$). Thus, the accuracy was computed considering the concentrations detected in spiked and nonspiked samples by using the following formula: $[\text{100} \times (\text{concentration}_{\text{spiked}} - \text{concentration}_{\text{nonspiked}}) / \text{spiked concentration}]$. On the other hand, the fractionation method was validated using standard solutions of bovine serum albumin (BSA), as described elsewhere.²⁶ For this purpose, we prepared a 50 mg/mL aqueous solution of BSA containing copper and zinc, which was subjected to the above-described protocol for protein precipitation under non-denaturing conditions. Then, multielemental analysis was performed in the resulting HMM and LMM fractions to check the integrity of metal-protein bindings during the extraction process (i.e., negligible release of copper and zinc into the LMM fraction).

2.5 | Statistical analysis

Multielemental data were preprocessed and statistically analyzed using the MetaboAnalyst 5.0 web tool (<https://www.metaboanalyst.ca/>). Before performing any statistical analysis, various preprocessing techniques were applied for enhancing the quality of the data matrix via removing unwanted variability sources. To this end, we first discarded variables with more than 20% missing values, and data imputation was then performed by applying the kNN algorithm. Afterward, the data were

log transformed and Pareto scaled to increase the symmetry of distributions and to adjust for dissimilarities in fold differences between the different variables under investigation, respectively. Data normality was evaluated through normal probability plots and the Kolmogorov-Smirnov test. Finally, clinical, biochemical, and multielemental data were subjected to Student's *t*-test to look for differences between the study groups. *p*-Values below 0.05 were considered as statistically significant.

3 | RESULTS

Obesity-related anthropometric variables (i.e., height, weight) were higher in pubertal children compared to prepubertal ones, but with similar *Z*-scores (Table 1). Furthermore, pubertal children showed increased blood insulin at baseline and along the OGTT, which was reflected in higher HOMA-IR scores ($p = 0.011$), AUCi ($p = 0.0017$), and mean insulin levels ($p = 0.00078$), without differences in glycemia. Puberty was also characterized by raised circulating contents of various hormones related to sexual maturation (i.e., IGF-1, FSH, LH, E2, T). Regarding iron metabolism-related parameters, pubertal subjects had increased transferrin ($p = 0.021$) and haptoglobin ($p = 0.022$) plasma levels, as well as higher TIBC ($p = 0.0033$). On the other hand, pubertal development was associated with lower levels of lipid peroxidation products (TBARS, $p = 0.0023$), and the same trend was observed for protein carbonyls without reaching statistical significance ($p = 0.09$). In contrast, catalase activity was over-expressed in older subjects ($p = 0.026$), whereas the activities of G6PDH ($p = 0.0032$) and 6PGDH ($p = 0.00012$) were blunted. Finally, pubertal children also exhibited diminished CRP levels ($p = 0.030$).

The application of a high throughput metallomics method enabled us to quantify the total contents of various essential elements (chromium, cobalt, copper, iron, manganese, molybdenum, selenium, zinc) and potentially toxic heavy metals (cadmium, lead) in plasma and erythrocyte samples of the study participants, as well as to characterize the metal fractions conforming the metalloproteome (i.e., HMM species) and the labile metal pool (i.e., LMM species) (Table 2). Metals in blood were majorly distributed in the HMM fraction, but other LMM species were also detected for most of the minerals under investigation, as previously reported.^{27,28} The comparison of the study groups evidenced that pubertal children had reduced plasma contents of total copper ($p = 0.0023$) and labile iron ($p = 0.030$), which was accompanied by increased levels of zinc ($p = 0.000094$), manganese ($p = 0.000014$), and molybdenum ($p = 0.0071$)

containing metalloproteins. Plasmatic LMM-Cr species also tended to increase during puberty development without reaching statistical significance ($p = 0.09$). On the other hand, pubertal children with obesity showed higher erythroid levels of total selenium ($p = 0.013$) and HMM-bound manganese ($p = 0.0050$).

Finally, sex-stratified analyses were performed to explore the possible occurrence of sex-dependent alterations in the variables under investigation. In general, similar trends were observed within male and female subjects in the above-mentioned puberty-related changes in insulinemia (Figure S1), hormones (Figure S2), iron metabolism-related variables (Figure S3), inflammatory and oxidative stress markers (Figure S4), plasma trace elements (Figure S5), and erythroid trace elements (Figure S6). In particular, sexual maturation in boys was mainly reflected in raised blood levels of testosterone, whereas girls showed an increase of 17 β -estradiol contents. Interestingly, the amelioration of inflammation, oxidative stress, and trace element disturbances (Figures S5 and S6) was found to be slightly sharpened within male participants.

4 | DISCUSSION

As expected by group definition, pubertal children with obesity had increased levels of sexual hormones (i.e., LH, FSH, E2, T) and IGF-1, as well as sharpened IR, when compared to younger subjects.^{6,7} Furthermore, we also found puberty to be inversely related to inflammation¹⁰ and oxidative stress.^{29,30} These findings could be explained by the modulatory effects that sexual hormones, and particularly estrogens, have against obesity-induced inflammation and oxidative stress. In this respect, it has been reported that estradiol treatment inhibits the activation and recruitment of macrophages in high fat diet-fed mice.³¹ Other plausible protective functions include the estrogen-mediated degradation of inflammatory-active components³² and the induction of anti-inflammatory components.³³ Similarly, sexual hormones have also demonstrated antioxidant functions by stimulating the expression and activity of catalase, superoxide dismutase, and glutathione peroxidase.^{8,9} This concurs with our results showing improved antioxidant capacity (i.e., raised catalase activity) and lower oxidative damage (i.e., reduced content of TBARS and protein carbonyls) within pubertal subjects. Supporting this rationale, we also found prepuberty to be characterized by an exacerbated reducing power generation by means of the pentose phosphate pathway, as reflected in increased G6PDH and 6PGDH activities. In the event of oxidative stress, this pathway can undergo an upregulation of up to

TABLE 1 Demographic, anthropometric, and biochemical characteristics of the study population.

	Prepubertal subjects	Pubertal subjects	p-Value
<i>Demographic and anthropometric variables</i>			
N	46	48	-
Age (years)	9.4 ± 1.4	12.7 ± 1.5	8.2 × 10 ⁻¹⁸
Sex (% male)	56.5	60.4	NS
Weight (kg)	59.0 ± 11.4	78.8 ± 18.8	2.0 × 10 ⁻⁸
Weight (Z-score)	5.1 ± 2.3	4.5 ± 1.9	NS
Body mass index (BMI, kg/m ²)	29.2 ± 4.1	31.0 ± 5.9	NS
Body mass index (Z-score)	4.7 ± 2.0	4.0 ± 2.0	NS
<i>Glucose and insulin metabolism</i>			
Glucose, t = 0 min (mg/dL)	86.0 ± 7.4	85.9 ± 10.0	NS
Glucose, t = 030 min (mg/dL)	129.9 ± 24.7	142.8 ± 24.2	NS
Glucose, t = 060 min (mg/dL)	133.1 ± 34.8	134.7 ± 26.9	NS
Glucose, t = 090 min (mg/dL)	124.7 ± 32.0	124.6 ± 27.8	NS
Glucose, t = 0120 min (mg/dL)	124.3 ± 28.2	122.3 ± 29.0	NS
Mean glucose (mg/dL)	121.7 ± 25.9	122.4 ± 19.6	NS
Area under the curve for glucose (AUC _G , mg·h/dL)	205.8 ± 57.6	210.2 ± 61.8	NS
Insulin, t = 00 min (μU/mL)	16.9 ± 7.5	23.1 ± 11.3	3.9 × 10 ⁻³
Insulin, t = 030 min (μU/mL)	130.0 ± 99.4	150.5 ± 96.7	3.3 × 10 ⁻²
Insulin, t = 060 min (μU/mL)	128.8 ± 73.9	158.2 ± 78.5	2.2 × 10 ⁻³
Insulin, t = 090 min (μU/mL)	125.5 ± 71.0	180.4 ± 137.9	2.9 × 10 ⁻³
Insulin, t = 0120 min (μU/mL)	117.2 ± 78.1	166.9 ± 112.8	3.3 × 10 ⁻³
Mean insulin (μU/mL)	103.1 ± 59.2	138.6 ± 67.3	7.8 × 10 ⁻⁴
Area under the curve for insulin (AUC _I , μU·h/mL)	220.3 ± 134.2	281.6 ± 142.0	1.7 × 10 ⁻³
HOMA-IR	3.6 ± 1.7	4.9 ± 2.6	1.1 × 10 ⁻²
<i>Lipid metabolism</i>			
Total cholesterol (mg/dL)	160.4 ± 33.3	167.4 ± 80.6	NS
Low-density lipoprotein cholesterol (mg/dL)	98.4 ± 30.3	93.6 ± 22.2	NS
High-density lipoprotein cholesterol (mg/dL)	44.7 ± 8.4	46.4 ± 27.2	NS
Triglycerides (mg/dL)	87.4 ± 42.7	108.5 ± 54.4	NS
<i>Hormonal profile</i>			
Growth hormone (ng/mL)	0.82 ± 1.6	0.97 ± 2.2	NS
Insulin-like growth factor 1 (IGF-1, ng/mL)	219.4 ± 100.3	371.3 ± 119.7	1.1 × 10 ⁻⁴
Follicle-stimulating hormone (FSH, mU/mL)	2.0 ± 1.9	4.5 ± 2.8	1.0 × 10 ⁻⁴
Luteinizing hormone (LH, mU/mL)	0.4 ± 1.3	3.8 ± 5.4	3.5 × 10 ⁻³
Testosterone (T, ng/dL)	16.1 ± 7.7	131.9 ± 134.5	6.1 × 10 ⁻⁵
17β-estradiol (E2, pg/mL)	20.7 ± 8.4	37.1 ± 28.7	1.0 × 10 ⁻²
<i>Iron metabolism</i>			
Ferritin (ng/mL)	45.6 ± 21.9	48.8 ± 30.2	NS
Transferrin (mg/dL)	303.2 ± 22.0	319.3 ± 30.9	2.1 × 10 ⁻²
Transferrin saturation (%)	18.5 ± 7.8	27.7 ± 64.6	NS
Total iron-binding capacity (TIBC, μg/dL)	380.4 ± 26.8	394.8 ± 37.2	3.3 × 10 ⁻³
Haptoglobin (mg/dL)	109.5 ± 32.3	133.5 ± 38.8	2.2 × 10 ⁻²

TABLE 1 (Continued)

	Prepubertal subjects	Pubertal subjects	p-Value
<i>Inflammation and oxidative stress</i>			
C-reactive protein (CRP, mg/L)	6.4 ± 7.9	3.3 ± 2.9	3.0 × 10 ⁻²
Thiobarbituric acid reactive substances (TBARS, nmol/mg protein)	3.1 ± 17	1.8 ± 1.1	2.3 × 10 ⁻³
Protein carbonyls (nmol/mg protein)	0.64 ± 0.67	0.56 ± 0.45	NS
Total antioxidant capacity (μmol Trolox/mg protein)	0.22 ± 0.08	0.21 ± 0.15	NS
Catalase activity (μmol H ₂ O ₂ /min mg protein)	3.4 ± 3.4	6.2 ± 6.9	2.6 × 10 ⁻²
Glutathione reductase activity (nmol NADP/min mg protein)	0.079 ± 0.056	0.074 ± 0.069	NS
Glucose-6-phosphate dehydrogenase activity (G6PDH, nmol NADPH/min mg protein)	13.6 ± 14.3	4.7 ± 6.0	3.2 × 10 ⁻³
6-Phosphogluconate dehydrogenase activity (6PGDH, nmol NADPH/min mg protein)	9.9 ± 9.8	2.4 ± 1.9	1.2 × 10 ⁻⁴

Note: Results are expressed as mean ± SD (except for sex, expressed as percentage).

Abbreviation: NS, nonsignificant.

20-fold to maintain and adequate redox control and avoid pathological consequences, as it has recently been described in childhood obesity.⁴ Thus, our observation of higher G6PDH and 6PGDH activities in the prepubertal group further pinpoints to the existence of an aggravated oxidative milieu at earlier ages.

Interestingly, this amelioration of obesity-related oxidative stress and inflammation during puberty was also reflected in a healthier metal profile in terms of reduced content of potentially toxic species and raised levels of essential elements. One of the most remarkable findings in this regard was the clearance of plasma labile iron levels among pubertal children. The same downward trend was observed for other redox-active metals in the LMM fraction (e.g., copper, manganese) without reaching statistical significance. In this respect, it should be noted that transition metals in the organism are usually found in the form of metalloproteins, but aberrant alterations in their homeostasis can lead to the release of free species. These free metal species may in turn undergo redox cycling reactions (e.g., Fenton reaction) to produce reactive oxygen species (ROS).³⁴ Although this is the first time, to our knowledge, that this condition is described in obesity, increased levels of free iron and copper have previously been reported in other diseases (e.g., Alzheimer's disease) as a result of impairments in some of the proteins that regulate their transport and storage.²⁸ In line with this rationale, we found prepubertal children to exhibit lower TIBC and reduced blood levels of transferrin, haptoglobin, and ferritin (this latter not significant), which are crucial protein regulators of iron homeostasis.³⁵ These differences could

be majorly driven by sexual hormones, in agreement with existing evidence proving their influence over the expression of multiple ferroproteins in different cells.^{36–38} Altogether, we hypothesize that puberty-induced improvement of iron metabolism (and other metals such as copper and manganese) would minimize the release of ROS-generating labile species and, therefore, contribute to better oxidative control.

Multielemental analysis also revealed a significant decline in the total plasma levels of copper during puberty, which was accompanied by increased content of zinc-containing proteins. In childhood obesity, the secretion of inflammatory cytokines by adipose tissue is known to induce intracellular copper efflux and zinc uptake, thereby leading to increased Cu/Zn ratios.^{15–17} In turn, this increment in copper levels may exacerbate oxidative stress because of its capacity to generate ROS, as discussed above. Therefore, the diminished Cu/Zn ratios that we observed among pubertal participants could be regarded as a direct reflection of the more effective inflammatory and oxidative resolution capacity that is developed along sexual maturation.

Puberty was also characterized by raised plasma levels of various trace elements that are directly involved in glucose and lipid metabolism, including the above-mentioned increase of zinc proteins, but also of molybdenum in the HMM fraction and chromium in the LMM fraction. On the one hand, zinc has been reported to play essential roles in the production, storage, and action of insulin.³⁹ Molybdenum is also known to participate in glucose-stimulated insulin secretion and

TABLE 2 Concentrations of metal and metalloid elements in the total, high molecular mass (HMM), and low molecular mass (LMM) fractions from plasma and erythrocyte samples.

		Plasma			Erythrocytes		
		Prepubertal subjects	Pubertal subjects	p-Value	Prepubertal subjects	Pubertal subjects	p-Value
Cadmium	Total	0.0034 ± 0.013	0.0029 ± 0.0089	NS	1.7 ± 2.1	1.9 ± 1.9	NS
	HMM	0.0031 ± 0.0098	0.0029 ± 0.0076	NS	1.6 ± 1.7	2.1 ± 2.7	NS
	LMM	ND	ND	-	ND	ND	-
Chromium	Total	5.8 ± 2.8	5.8 ± 3.1	NS	ND	ND	-
	HMM	6.0 ± 3.9	5.7 ± 3.6	NS	ND	ND	-
	LMM	1.02 ± 1.27	1.72 ± 3.37	NS	ND	ND	-
Cobalt	Total	1.7 ± 1.1	1.8 ± 2.3	NS	ND	ND	-
	HMM	0.72 ± 0.24	0.76 ± 0.30	NS	ND	ND	-
	LMM	0.31 ± 0.062	0.30 ± 0.055	NS	ND	ND	-
Copper	Total	1475.2 ± 234.7	1295.7 ± 231.9	2.3 · 10 ⁻³	606.8 ± 139.0	658.5 ± 259.8	NS
	HMM	1294.2 ± 181.5	1241.5 ± 177.0	NS	608.9 ± 754.8	673.3 ± 560.4	NS
	LMM	28.8 ± 34.2	20.2 ± 17.2	NS	1.6 ± 0.6	2.0 ± 1.6	NS
Iron	Total	755.3 ± 315.8	711.9 ± 401.2	NS	540889.9 ± 92998.9	561019.0 ± 134730.6	NS
	HMM	734.5 ± 266.7	747.4 ± 358.0	NS	535862.3 ± 94481.7	482818.0 ± 126812.5	NS
	LMM	32.2 ± 27.2	23.7 ± 10.8	3.0 · 10 ⁻²	19.6 ± 8.4	22.9 ± 12.7	NS
Lead	Total	0.023 ± 0.0053	0.023 ± 0.0022	NS	65.7 ± 18.5	60.3 ± 46.1	NS
	HMM	0.022 ± 0.0043	0.023 ± 0.0049	NS	64.6 ± 80.7	53.3 ± 56.3	NS
	LMM	ND	ND	-	1.3 ± 0.2	1.4 ± 0.6	NS
Manganese	Total	4.1 ± 4.8	4.1 ± 5.5	NS	25.8 ± 50.6	39.5 ± 87.0	NS
	HMM	3.8 ± 1.0	4.5 ± 0.5	1.4 · 10 ⁻⁵	23.7 ± 6.7	33.8 ± 18.3	5.0 × 10 ⁻³
	LMM	0.51 ± 0.60	0.18 ± 0.21	NS	0.66 ± 0.15	0.62 ± 0.18	NS
Molybdenum	Total	2.7 ± 0.8	2.4 ± 0.7	NS	29.8 ± 39.6	40.6 ± 117.9	NS
	HMM	2.0 ± 0.6	2.3 ± 0.7	7.1 · 10 ⁻³	34.9 ± 25.8	37.3 ± 27.1	NS
	LMM	ND	ND	-	0.22 ± 0.12	0.25 ± 0.23	NS
Selenium	Total	125.1 ± 18.8	121.5 ± 21.1	NS	161.9 ± 58.7	184.9 ± 78.8	1.3 × 10 ⁻²
	HMM	134.9 ± 16.7	137.6 ± 19.1	NS	156.0 ± 126.1	175.9 ± 199.9	NS
	LMM	2.3 ± 3.6	1.8 ± 1.4	NS	0.19 ± 0.13	0.19 ± 0.14	NS
Zinc	Total	793.3 ± 412.9	775.3 ± 243.3	NS	9485.1 ± 1742.4	9879.2 ± 2385.5	NS
	HMM	727.5 ± 327.1	965.2 ± 292.4	9.4 · 10 ⁻⁵	9332.7 ± 4808.4	8339.6 ± 3741.2	NS
	LMM	31.6 ± 14.2	37.2 ± 14.4	NS	61.2 ± 6.8	62.4 ± 11.0	NS

Note: Results are expressed as mean ± SD (µg/L).

Abbreviations: ND, nondetected; NS, nonsignificant.

signaling, to modulate glucose metabolism, and to mitigate lipid peroxidation and accumulation. Similarly, chromium has demonstrated positive effects on blood glucose control and the prevention of atherogenic dyslipidemia, being the low-molecular-weight chromium-binding substance the major active form of this micronutrient.³⁹ Thus, the increment of these essential elements in the blood of pubertal children could be indicative of the close inter-relationship between oxidative stress and insulin metabolism. In this vein, it is

well recognized that a pro-oxidant environment may considerably perturb metabolic control (e.g., by provoking β-cell dysfunction) in obesity and related comorbidities. Accordingly, our results suggest that puberty provides children with obesity a set of adaptive tools (i.e., proper trace element status) to fight against IR-related impairments.

Finally, we also observed higher concentrations of various antioxidant metal species in pubertal children, namely manganese-containing proteins (in plasma and

erythrocytes) and total erythroid selenium. Noteworthy, children with obesity have been described to be characterized by reduced activity and content of Se- and Mn-dependent antioxidant enzymes, such as glutathione peroxidase⁴ and manganese superoxide dismutase.⁴⁰ It has also been reported that proper maintenance of their homeostasis is crucial for mitigating oxidative processes that may worsen insulin secretion³⁹ and for alleviating inflammatory signaling pathways.^{41,42} Altogether, these results further reinforce our hypothesis about the central role that trace elements may play in puberty-related amelioration of oxidative stress and inflammation.

The main strength of this study was the use of a well-characterized population consisting of prepubertal and pubertal subjects with obesity, from whom blood samples were collected with the aim of complementarily determining the multielemental profile and classical biomarkers of oxidative stress and inflammation. This enabled us to comprehensively characterize a wide number of potentially inter-related variables, including markers of oxidative stress and inflammation, biochemical profile (insulin, glucose, lipids), hormonal status, and circulating trace elements. Furthermore, we employed a high-throughput method for size-fractionation of metal species to simultaneously determine the total content of various essential and toxic elements, as well as to differentiate between metalloproteins and labile species. This is of utmost importance considering that the chemical form in which metals are present in the organism has a great impact on their toxicological properties, biological activity, and mobility across biological compartments. Herein, it is also noteworthy the parallel investigation of plasma and erythrocyte samples with the aim of investigating the bio-distribution of trace elements in a multicompartamental manner, that is, at circulating and cellular levels. In this respect, erythrocytes have been proposed as powerful systemic indicators of the metabolic and redox status of the organism. However, some limitations deserve to be mentioned as well. The major limitation of this study was the lack of prospective data to evaluate longitudinal changes in the variables under investigation along pubertal development. The relatively small sample size and the lack of an independent validation cohort would make necessary future research in larger populations to corroborate our findings. In this respect, the enrollment of sex-stratified populations could be of great interest to get deeper insights into the potential occurrence of sexual dimorphisms in the impact of puberty on obesity-related complications. Finally, it is also worth mentioning that only one inflammatory marker (i.e., CRP) was determined in the study population, which hindered establishing robust associations between metal alterations and the low-grade chronic inflammation that is typically observed in childhood obesity.

5 | CONCLUSIONS

In this study, we have delved into the influence that puberty exerts over the most relevant complications of obesity, namely oxidative stress and inflammation, and their association with trace element status. Herein, we proved pubertal children with obesity to exhibit a better oxidative and inflammatory control, in relation with a healthier multielemental profile. In particular, puberty was characterized by increased levels of essential elements involved in the antioxidant defense and metabolic control (selenium, manganese, zinc, molybdenum) and decreased content of potentially deleterious species (copper, labile iron). Accordingly, we hypothesize that pubertal development might trigger among children a set of trace element-mediated buffering mechanisms aimed to fight against obesity-related complications. However, future studies are needed to better understand this interplay between metals, obesity, and puberty, as well as to elucidate the underlying mechanisms.

AUTHOR CONTRIBUTIONS

Conceptualization: Raúl González-Domínguez. *Data curation:* Álvaro González-Domínguez and Raúl González-Domínguez. *Formal analysis:* Álvaro González-Domínguez, María Millán-Martínez, and Raúl González-Domínguez. *Funding acquisition:* Raúl González-Domínguez, Rosa María Mateos-Bernal and Alfonso María Lechuga-Sancho. *Investigation:* Álvaro González-Domínguez, María Millán-Martínez, Jesús Domínguez-Riscart, Alfonso María Lechuga-Sancho, and Raúl González-Domínguez. *Methodology:* María Millán-Martínez and Raúl González-Domínguez. *Project administration:* Raúl González-Domínguez. *Resources:* Raúl González-Domínguez and Alfonso María Lechuga-Sancho. *Supervision:* Raúl González-Domínguez. *Roles/Writing—original draft:* Álvaro González-Domínguez and Raúl González-Domínguez. *Writing—review & editing:* Álvaro González-Domínguez, María Millán-Martínez, Jesús Domínguez-Riscart, Rosa María Mateos-Bernal Alfonso María Lechuga-Sancho, and Raúl González-Domínguez. All authors have read and agreed to the published version of the manuscript.

FUNDING INFORMATION

This research was funded by the Spanish Government through Instituto de Salud Carlos III (PI22/01899, PI18/01316). Álvaro González-Domínguez is supported by an intramural grant from the Biomedical Research and Innovation Institute of Cádiz (LII19/16IN-CO24), and Raúl González-Domínguez is recipient of a “Miguel Servet” fellowship funded by Instituto de Salud Carlos III (CP21/00120).

CONFLICT OF INTEREST STATEMENT

The authors declare that they have no competing interests.

DATA AVAILABILITY STATEMENT

The datasets used and/or analyzed during the current study are available from the corresponding author on reasonable request.

ORCID

Rosa María Mateos-Bernal  <https://orcid.org/0000-0002-9853-1103>

Raúl González-Domínguez  <https://orcid.org/0000-0002-7640-8833>

REFERENCES

- World Health Organization. <https://www.who.int/dietphysicalactivity/childhood/en/>. Revised November, 2022.
- Goran MI, editor. Childhood obesity: causes, consequences, and intervention approaches. Boca Raton, FL: CRC Press; 2016.
- Mărginean CO, Meliș LE, Huțanu A, Ghiga DV, Săsăran MO. The adipokines and inflammatory status in the era of pediatric obesity. *Cytokine*. 2020;126:154925.
- González-Domínguez Á, Visiedo F, Domínguez-Riscart J, Ruiz-Mateos B, Saez-Benito A, Lechuga-Sancho AM, et al. Blunted reducing power generation in erythrocytes contributes to oxidative stress in Prepubertal obese children with insulin resistance. *Antioxidants*. 2021;10:244.
- González-Domínguez Á, Visiedo F, Domínguez-Riscart J, Durán-Ruiz MC, Saez-Benito A, Lechuga-Sancho AM, et al. Catalase post-translational modifications as key targets in the control of erythrocyte redox homeostasis in children with obesity and insulin resistance. *Free Radic Biol Med*. 2022;191:40–7.
- Wood CL, Lane LC, Cheetham T. Puberty: Normal physiology (brief overview). *Best Pract Res Clin Endocrinol Metab*. 2019; 33:101265.
- Kelsey MM, Zeitler PS. Insulin resistance of puberty. *Curr Diab Rep*. 2016;16:64.
- Tower J, Pomatto LCD, Davies KJA. Sex differences in the response to oxidative and proteolytic stress. *Redox Biol*. 2020; 31:101488.
- Cruz-Topete D, Dominic P, Stokes KY. Uncovering sex-specific mechanisms of action of testosterone and redox balance. *Redox Biol*. 2020;31:101490.
- Stumper A, Moriarity DP, Coe CL, Ellman LM, Abramson LY, Alloy LB. Pubertal status and age are differentially associated with inflammatory biomarkers in female and male adolescents. *J Youth Adolesc*. 2020;49:1379–92.
- Zoroddu MA, Aaseth J, Crisponi G, Medici S, Peana M, Nurchi VM. The essential metals for humans: a brief overview. *J Inorg Biochem*. 2019;195:120–9.
- Wang C, Zhang R, Wei X, Lv M, Jiang Z. Metalloimmunology: the metal ion-controlled immunity. *Adv Immunol*. 2020;145: 187–241.
- Stevenson MJ, Uyeda KS, Harder NHO, Heffern MC. Metal-dependent hormone function: the emerging interdisciplinary field of metalloendocrinology. *Metallomics*. 2019;11:85–110.
- Thillan K, Lanerolle P, Thoradeniya T, Samaranyake D, Chandrajith R, Wickramasinghe P. Micronutrient status and associated factors of adiposity in primary school children with normal and high body fat in Colombo municipal area, Sri Lanka. *BMC Pediatr*. 2021;21:14.
- Fan Y, Zhang C, Bu J. Relationship between selected serum metallic elements and obesity in children and adolescent in the U.S. *Nutrients*. 2017;9:104.
- Azab SF, Saleh SH, Elsaed WF, Elshafie MA, Sherief LM, Esh AM. Serum trace elements in obese Egyptian children: a case-control study. *Ital J Pediatr*. 2014;40:20.
- González-Domínguez Á, Millán-Martínez M, Domínguez-Riscart J, Mateos RM, Lechuga-Sancho AM, González-Domínguez R. Altered metal homeostasis associates with inflammation, oxidative stress, impaired glucose metabolism, and dyslipidemia in the crosstalk between childhood obesity and insulin resistance. *Antioxidants*. 2022;11:2439.
- González-Domínguez Á, Domínguez-Riscart J, Millán-Martínez M, Lechuga-Sancho AM, González-Domínguez R. Exploring the association between circulating trace elements, metabolic risk factors, and the adherence to a Mediterranean diet among children and adolescents with obesity. *Front Public Health*. 2023;10:1016819.
- Hernández M, Castellet J, Narvaiza J, Rincón J, Ruiz I, Sánchez E, et al. Curvas y tablas de crecimiento (0-18 años). In: Instituto de Investigación Sobre Crecimiento y Desarrollo. 1988. p. 1–32.
- Erel O. A novel automated direct measurement method for total antioxidant capacity using a new generation, more stable ABTS radical cation. *Clin Biochem*. 2004;37:277–85.
- Buege JA, Aust SD. Microsomal lipid peroxidation. *Methods Enzymol*. 1978;52:302–10.
- Levine RL, Garland D, Oliver CN, Amici A, Climent I, Lenz A-G, et al. Determination of carbonyl content in oxidatively modified proteins. *Methods Enzymol*. 1990;186:464–78.
- Aebi H. Catalase in vitro. *Methods Enzymol*. 1984;105:121–6.
- Mohanty JG, Nagababu E, Rifkind JM. Red blood cell oxidative stress impairs oxygen delivery and induces red blood cell aging. *Front Physiol*. 2014;5:84.
- González-Domínguez Á, Millán-Martínez M, Sánchez-Rodas D, Lechuga-Sancho AM, González-Domínguez R. Characterization of the plasmatic and erythroid multielemental bio-distribution in childhood obesity using a high-throughput method for size fractionation of metal species. In: González-Domínguez R, editor. *Mass spectrometry for metabolomics (methods in molecular biology)*. New York: Humana; 2023. p. 123–32.
- González-Domínguez R. Size-fractionation of metal species from serum samples for studying element biodistribution in Alzheimer's disease. In: White AR, editor. *Metals in the brain: measurement and imaging (Neuromethods)*. New York: Humana Press; 2017. p. 127–49.
- González-Domínguez R, García-Barrera T, Gómez-Ariza JL. Homeostasis of metals in the progression of Alzheimer's disease. *Biomaterials*. 2014;27:539–49.
- González-Domínguez R, García-Barrera T, Gómez-Ariza JL. Characterization of metal profiles in serum during the progression of Alzheimer's disease. *Metallomics*. 2014;6:292–300.
- Faienza MF, Francavilla R, Goffredo R, Ventura A, Marzano F, Panzarino G, et al. Oxidative stress in obesity and metabolic



- syndrome in children and adolescents. *Horm Res Paediatr*. 2012;78:158–64.
30. Rupérez AI, Mesa MD, Anguita-Ruiz A, González-Gil EM, Vázquez-Cobela R, Moreno LA, et al. Antioxidants and oxidative stress in children: influence of puberty and metabolically unhealthy status. *Antioxidants*. 2020;9:618.
 31. Varghese M, Griffin C, Singer K. The role of sex and sex hormones in regulating obesity-induced inflammation. In: Mauvais-Jarvis F, editor. *Sex and gender factors affecting metabolic homeostasis, diabetes and obesity (advances in experimental medicine and biology)*. Cham: Springer; 2017. p. 65–86.
 32. Kim M, Neinast MD, Frank AP, Sun K, Park J, Zehr JA, et al. ER α upregulates Phd3 to ameliorate HIF-1 induced fibrosis and inflammation in adipose tissue. *Mol Metab*. 2014;3:642–51.
 33. Draijer C, Hylkema MN, Boersma CE, Klok PA, Robbe P, Timens W, et al. Sexual maturation protects against development of lung inflammation through estrogen. *Am J Physiol Lung Cell Mol Physiol*. 2016;310:L166–74.
 34. Valko M, Jomova K, Rhodes CJ, Kuča K, Musilek K. Redox and non-redox-metal-induced formation of free radicals and their role in human disease. *Arch Toxicol*. 2016;90:1–37.
 35. González-Domínguez Á, Visiedo-García FM, Domínguez-Riscart J, González-Domínguez R, Mateos RM, Lechuga-Sancho AM. Iron metabolism in obesity and metabolic syndrome. *Int J Mol Sci*. 2020;21:5529.
 36. Qu Y, Li N, Xu M, Zhang D, Xie J, Wang J. Estrogen upregulates iron transporters and iron storage protein through hypoxia inducible factor 1 alpha activation mediated by estrogen receptor β and G protein estrogen receptor in BV2 microglia cells. *Neurochem Res*. 2022;47:3659–69.
 37. Xu M, Tan X, Li N, Wu H, Wang Y, Xie J, et al. Differential regulation of estrogen in iron metabolism in astrocytes and neurons. *J Cell Physiol*. 2019;234:4232–42.
 38. Guo W, Bachman E, Li M, Roy CN, Blusztajn J, Wong S, et al. Testosterone administration inhibits hepcidin transcription and is associated with increased iron incorporation into red blood cells. *Aging Cell*. 2013;12:280–91.
 39. Barra NG, Anê FF, Cavallari JF, Singh AM, Chan DY, Schertzer JD. Micronutrients impact the gut microbiota and blood glucose. *J Endocrinol*. 2021;250:R1–R21.
 40. Mohseni R, Arab Sadeghabadi Z, Goodarzi MT, Teimouri M, Nourbakhsh M, Razzaghy AM. Evaluation of Mn-superoxide dismutase and catalase gene expression in childhood obesity: its association with insulin resistance. *J Pediatr Endocrinol Metab*. 2018;31:727–32.
 41. Fontenelle LC, Cardoso de Araújo DS, da Cunha ST, Climaco Cruz KJ, Henriques GS, do Nascimento Marreiro D. Nutritional status of selenium in overweight and obesity: a systematic review and meta-analysis. *Clin Nutr*. 2022;41:862–84.
 42. Li L, Yang X. The essential element manganese, oxidative stress, and metabolic diseases: links and interactions. *Oxid Med Cell Longev*. 2018;2018:1–11.

SUPPORTING INFORMATION

Additional supporting information can be found online in the Supporting Information section at the end of this article.

How to cite this article: González-Domínguez Á, Domínguez-Riscart J, Millán-Martínez M, Mateos-Bernal RM, Lechuga-Sancho AM, González-Domínguez R. Trace elements as potential modulators of puberty-induced amelioration of oxidative stress and inflammation in childhood obesity. *BioFactors*. 2023. <https://doi.org/10.1002/biof.1946>